Desorption of Nitric Acid From Boehmite and Gibbsite

M. W. Ross and T. C. DeVore*

Department of Chemistry, James Madison University, MSC 4501, Harrisonburg, Virginia 22807

Received: November 20, 2007; Revised Manuscript Received: May 5, 2008

Solid-state Fourier transform infrared spectroscopy (FTIR), evolved gas analysis-FTIR (EGA-FTIR), thermal gravimetric analysis (TGA), and differential scanning calorimetry (DSC) have been used to investigate the desorption of nitric acid from boehmite and from gibbsite. Samples containing between 3 and 36% of adsorbed nitric acid by mass were prepared by placing the mineral in a 70% nitric acid solution or by the adsorption of nitric acid vapors in humid air. FTIR established that water-solvated nitrate was the main species adsorbed on the surface of either mineral under these conditions. The water-solvated nitrate vaporized as nitric acid at ~400 K with an enthalpy of desorption of ~50 kJ/mol for both surfaces. A second nitric acid desorption occurred at ~450 K and had an enthalpy of desorption of 85 kJ/mol (95 kJ/mol) for boehmite (gibbsite). This was assigned as desorption of partially solvated aluminum hydroxylated nitrate. Monodentate and bridging nitrate were also observed on the boehmite. These species desorbed at ~725 K as NO_2 and O_2 with an enthalpy of reaction of ~55 kJ/mol of NO_2 desorbed.

Introduction

NO_x, a component of photochemical smog and a catalyst for the stratospheric destruction of ozone, is added to the atmosphere from natural sources such as lightening strikes and man-made sources such as automobile exhaust.[1,2] After air oxidation, NO_x reacts with water to form nitric acid, a constituent of acid rain. Since the concentrations of NO_x found in the atmosphere are generally less than that predicted based upon amounts released from the various sources, mineral aerosols have been suggested as a possible sink for NO_x, and Dentener et al. have calculated that more than 40% of the total atmospheric nitrate could be adsorbed on them.[3] Mineral aerosols are produced by wind-blown soils and contain minerals such as alumina, silica, and titania. One component of mineral aerosol particles, alumina, is also the most commonly used support material in traditional three-way catalysts designed to remove NO_x from auto exhausts.[1,2] Hence, the interactions between alumina and NO_x contribute to the removal of NO_x at a main source as well as removing it in the environment.

Several investigations of the interactions between various forms of aluminum oxide and NO_x and/or nitric acid have now been reported.[1–13] Venkov et al. identified IR frequencies for coordinated nitrite and nitrate species during their investigation of NO and NO + O_2 adsorbed on γ-alumina.[4] Westerberg and Fridell determined that the bond strength between the alumina surface and the nitrate ions increased in the order of bidentate < monodentate < bridging from the intensity changes in the IR bands observed by heating a sample of NO_2 on γ-Al_2O_3 to temperatures between 373 and 673 K.[5] They measured the enthalpy of reaction for the monodentate−bridged transition and the monodentate−bidentate transition as −7.7 and +7.4 kJ/mol, respectively. Huang et al. observed NO desorption features at 370, 680, and 800 K in the temperature-programmed desorption (TPD) of a sample produced by exposing γ-Al_2O_3 to NO.[6] The 800 K feature was assigned as the decomposition of bidentate nitrate.[6] Goodman et al. determined that the amount of NO_2 adsorbed on γ-Al_2O_3 was directly dependent on the partial pressure of NO_2 in the system.[7] The chelating bridging nitrito species formed initially, with the monodentate, bidentate, and bridging nitrates being formed at high NO_2 coverage. Each of these investigations was conducted without co-adsorbed water.

There has been growing interest in the effect of co-adsorbed water on the adsorption of nitrate on alumina. Szanyi et al. discovered that small amounts of water converted bridging nitrates into monodentate nitrates, and higher water coverages produced water-solvated nitrate for NO_2 on γ-Al_2O_3.[8] Since even carefully dried samples contained some water, they assigned the NO_2 desorption peak at 722 K to the decomposition of solvated nitrate. Goodman et al. assigned an IR band at 1643 cm^{-1} as the ν_2 bending mode of adsorbed water and bands at 1350 and 1399 cm^{-1} as adsorbed solvated nitric acid for samples produced by depositing nitric acid on α-Al_2O_3 in the presence of water vapor.[9] Borensen et al. assigned IR bands between 1250 and 1500 cm^{-1} to the split ν_3 band of the nitrate ion for samples produced when γ-alumina was exposed to nitric acid vapors but found no evidence for surface-adsorbed solvated nitrate.[10,11] Although the proposed reaction pathways differed slightly, both investigations found evidence that surface hydroxyls contributed to the formation of surface nitrates. Baltrusaitis et al. observed IR bands at 1348 and 1406 cm^{-1} when water vapor was added to α-alumina or γ-alumina that had previously been exposed to nitric acid vapor.[12] Theoretical calculations using density functional theory indicated that these bands were from water-solvated nitrate. They identified two forms of solvated nitrate that they described as inner- and outer-sphere nitrate coordination. The difference in coordination was produced by the proximity of the nitrate ions to the surface.[12]

There have also been several investigations of the adsorption of nitric acid on minerals containing alumina.[11,13–17] Grassian and co-workers measured the uptake of nitric acid on Gobi dust and Saharan sand under relatively dry conditions.[13–15] They found that models using gas diffusion into underlying layers of powdered samples were needed to accurately account for the uptake of nitric acid. Even small amounts of water significantly increased the uptake of nitric acid by these particles. Seisel et al. used DRIFTS and a Knudsen cell reactor to measure the IR

* To whom correspondence should be addressed.

10.1021/jp7110555 CCC: $40.75
Published on Web 06/27/2008

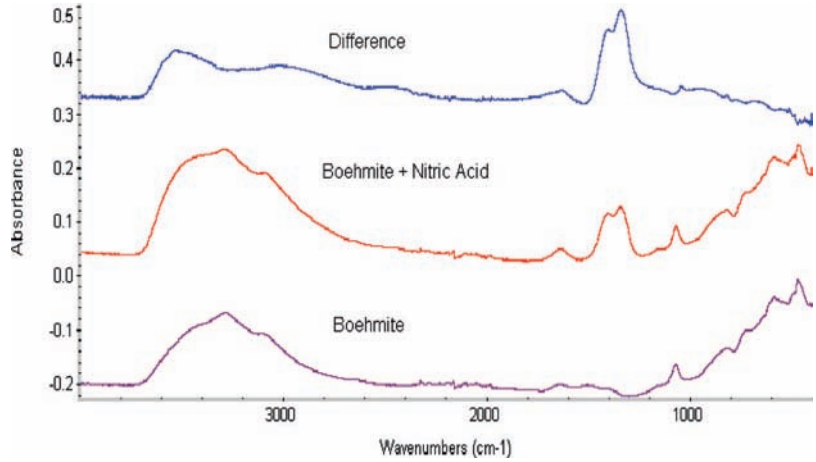

Figure 1. The IR spectra observed for boehmite and 20% nitric acid on boehmite. The difference spectrum shows the bands that formed when nitric acid was added.

spectra of the adsorbed species and to do kinetic studies on the rates of gas uptake for nitric acid on mineral dust.[11] They found a rapid adsorption of gas-phase nitric acid followed by a slower surface reaction between adsorbed nitric acid and surface OH groups. Oxide-coordinated bidentate frequencies at 1216 and 1556 cm^{-1} were reported for NO_3^- adsorbed on the mineral dust. Vlasenko et al. investigated the effect of humidity on the uptake kinetics of nitric acid by Arizona test dust and found that the rate increased nearly 10 fold as the relative humidity increased from 12 to 73%.[16] Angelini et al. reported the adsorption of nitric acid on dry and wet kaolinite and pyrophyllite.[17] They identified HNO_3 molecularly adsorbed on the aluminum hydroxide surface as well as irreversibly adsorbed monodentate, bidentate, bridged, and water-coordinated species.

The interactions between AlOOH (boehmite)/nitric acid and $Al(OH)_3$ (gibbsite)/nitric acid have been investigated using attenuated total reflectance-FTIR (ATR-FTIR) to determine the products formed and evolved gas analysis-FTIR (EGA-FTIR), thermogravimetric analysis (TGA), and differential scanning calorimetry (DSC) to investigate the stabilities of the species formed. Since humidity has been shown to affect the rate of adsorption, samples were prepared in air to mimic conditions found in the environment and to help determine if other components of the atmosphere would influence interactions between nitric acid and the surface. Water and nitric acid were also co-adsorbed to investigate the interactions in high-humidity environments.

Experimental Section

Materials. The boehmite (AlOOH) was Baker Chromatographic grade powder, and the gibbsite ($Al(OH)_3$) was from Fisher. Both were used as received. After confirming the identity of each using powder x-ray diffraction, the surface areas were determined by drying the sample in vacuum at 450 K to remove surface-adsorbed gases, adding excess water vapor to the system, placing the sample in vacuum at room temperature for 60 minutes to remove the weakly bound water vapor, and then measuring the mass loss when the adsorbed water was removed by heating the sample to 450 K in vacuum. The surface area determined for boehmite was 62 ± 5 m^2/g. Gibbsite had a surface area of 5 ± 2 m^2/g. Concentrated (70%) nitric acid and concentrated (95%) sulfuric acid solutions were obtained from Fisher and used as received.

Saturation with Nitric Acid. One dm^3 of 70% M nitric acid was carefully poured over 1 g of the solid aluminum compound and mixed to completely wet the surface. The excess liquid was allowed to evaporate in air for at least 12 hours prior to use. Once the excess nitric acid solution had evaporated, the samples were free-flowing, dry-appearing powders. Multiple applications of nitric acid solution were used to increase the amount of nitric acid adsorbed on the surface.

Exposure of the aluminum compounds to nitric acid vapor was done by supporting a polyethylene weigh boat containing ~1 g of the aluminum oxide on top of a 50 cm^3 beaker. The supported sample was placed in a 2 dm^3 beaker, and approximately 25 cm^3 of a 3:1 mixture of concentrated sulfuric acid/concentrated nitric acid was placed in the bottom of the beaker, and the beaker was covered with a watch glass to contain the vapor. Exposure times between 1 and 24 h were used to prepare samples containing a range in the amounts of adsorbed nitric acid.

The amount of nitric acid added to the sample was determined using thermal gravimetric analysis. Multiple exposures to nitric acid produced samples containing up to 36% of nitric acid by mass. Much of this could be removed by placing the sample in vacuum (~1 Pa) at 300 or 375 K. After 60 min at 375 K, the sample typically contained ~5% of nitric acid by mass. Samples are identified by their mass percents. For example, a sample that contained ~20% of nitric acid by mass is referred to as 20% nitric acid. All 5% nitric acid samples used here were produced by heating the sample in vacuum at 375 K. The 5% samples used for TGA, DSC, and FTIR analysis were removed from the vacuum and exposed to the atmosphere to load the samples into the instruments. Most samples were not removed from the vacuum for the EGA-FTIR analysis.

Solid-State IR. IR spectra were obtained using a Nicolet Smart Golden Gate ATR placed in the sample compartment of a Nicolet Avatar 6700 FTIR. The powdered sample was placed into the sample compartment of the ATR cell, and 100 scans at 1 cm^{-1} resolution were used to obtain the spectrum from 600−4000 cm^{-1}. They were processed and analyzed using the absorbance mode in the software. No attempts to determine accurate quantitative measurements were made using this data. Although dried nitrogen was flowed through the spectrometer and the bottom of the ATR cell, the sample compartment was exposed to the atmosphere. An empty cell was used as the background.

Powder X-Ray Diffraction. Powder x-ray diffraction was done using a Panalytical X'pert Pro. The pattern was obtained for 2θ from 5 to 80 degrees using Cu Kα radiation. The Powder

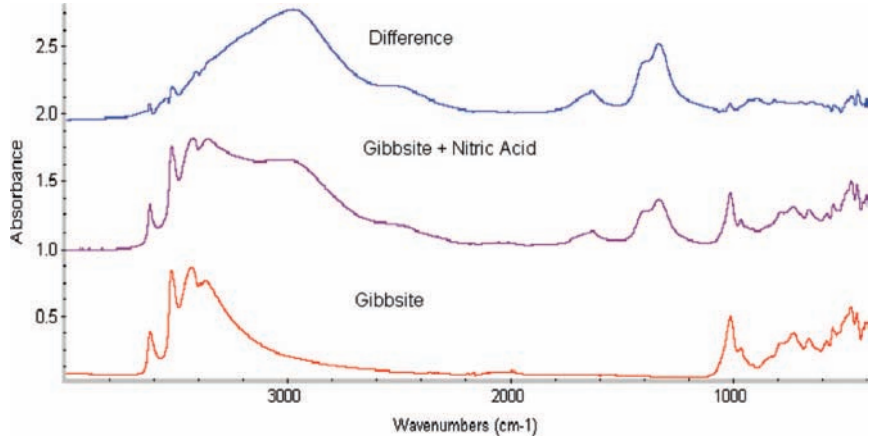

Figure 2. The IR spectra observed for gibbsite and 20% nitric acid on gibbsite. The difference spectrum shows the bands that formed when nitric acid was added.

TABLE 1: IR Bands (in cm^{-1}) Observed for the Deposition of Nitric Acid on Boehmite and Gibbsite after Heating the Sample to the Indicated Temperature in Vacuum

boehmite	gibbsite	assignment
	Temperature = 300 K	
820	815	ν_2 NO_3^-
1045	1045	ν_1 NO_3^-
1335	1337	NO_3^- co-adsorbed with H_2O
1405	1404	(outer sphere)
1633	1634	ν_2 H_2O
	1660	molec. adsorbed HNO_3
2457	2518	$\nu_{1,3}$ $H_{2n+1}O_n^+$?
2991	2990	$\nu_{1,3}$ $H_{2n+1}O_n^+$?
3525		$\nu_{1,3}$ H_2O
	Temperature = 375 K	
1335	1350	ν_3 NO_3^- co-adsorbed with H_2O
1410	1415	Al hydroxylated nitrate
1648	1649	ν_2 H_2O
	Temperature = 475 K	
1323	1325	ν_3 NO_3^- bridged/ monodentate
1418	1423	ν_3 partially solvated Al hydroxylated NO_3^-
1509	1520	ν_3 NO_3^- monodentate
1630	1608	ν_3 NO_3^- bridged
	Temperature = 675 K	
1276	1273	ν_3 NO_3^- bridged
1311	1309	ν_3 NO_3^- monodentate
1417		ν_3 partially solvated Al hydroxylated NO_3^-
1546	1557	ν_3 NO_3^- monodentate
1610	1608	ν_3 NO_3^- bridged

Diffraction Files (PDF) and the Cambridge Structural Database (CSD) were used to identify the diffraction patterns.

Temperature-Programmed Desorption (TPD). Temperature-programmed desorption was done in flowing nitrogen using a Mettler Toledo TGA/SDTA 851[e]. These investigations were done by placing 10 mg of sample into a 70 μL capped alumina crucible. Heating rates of 5, 10, 15, and 20°/min were used and a 40 mL/min flow of dry nitrogen was used as the carrier gas.

TGA was also used to obtain isothermal desorption curves under pseudo-Knudsen cell conditions. These experiments were done by placing 10 mg of compound in 70 μL capped alumina crucibles. The samples were heated to the desired temperature, and the isothermal mass loss was measured for 60 min. Since under ideal conditions the rate of mass loss would be linear with time and proportional to the equilibrium vapor pressure,[18] the natural logarithm of the slope of the linear portion of the mass verses time curve was then plotted verses the reciprocal of the absolute temperature to estimate the desorption enthalpy.

TPD in vacuum was done using a home-built EGA-FTIR apparatus that has been described in detail previously.[19–21] The cell was constructed by using o-ring connectors to attach KBr windows to two opposing arms of an MDC Corp. four-way cross stainless steel vacuum flange. One of the remaining arms of the flange was connected to the vacuum pump, and the final arm was connected to the sample tube. The sample tube was made from a 25 cm long piece of 9 mm OD glass tubing that had been closed on one end. A furnace assembly, made by wrapping nichrome wire around a 12 mm OD quartz tube, was used to heat the sample. The temperature of the furnace was controlled using a BK Precision high-current DC-regulated power supply and was measured with a chromel−alumel thermocouple connected to a Fluke digital thermometer.

A ~0.5 g sample was used for the EGA-FTIR investigations. Most samples were out-gassed under vacuum (~100 millitorr) at 375 K for up to 60 min to remove the excess nitric acid immediately prior to use. The sample was then heated at a rate of 4−6 K/min from 375 to 800 K. The evolved gases were drawn into the cell by the vacuum and monitored using a Nicolet 6700 FTIR. This spectrometer was set to collect and store one spectrum every 2 seconds for reaction times up to 60 min. Spectra were collected from 400 to 4000 cm^{-1} with 4 cm^{-1} resolution. Since the vacuum pulled the sample through the cell, no carrier gases were used in these experiments. The evolved gases were identified by matching the observed IR spectrum to spectra available in the Nicolet Aldrich spectral library.

Differential Scanning Calorimetry (DSC). DSC was obtained using a Mettler Toledo DSC822[e]. A 10 mg sample was placed in a sealed aluminum pan and heated at 10 K/min in static air. An empty aluminum pan was used as the reference.

Results and Discussion

Solid State IR. The IR spectra obtained for boehmite, 20% nitric acid on boehmite, and the difference spectrum obtained by subtracting the boehmite spectrum from the 20% nitric acid spectrum are presented in Figure 1. A similar set of spectra for 20% nitric acid on gibbsite are presented in Figure 2. The bands observed in the difference spectrum and the assignments for each are summarized in Table 1. The bands at 820 (815), 1045 (1045), 1335 (1337), and 1405 cm^{-1} (1398 cm^{-1}) for nitric acid adsorbed on boehmite (gibbsite) agreed well with the IR bands

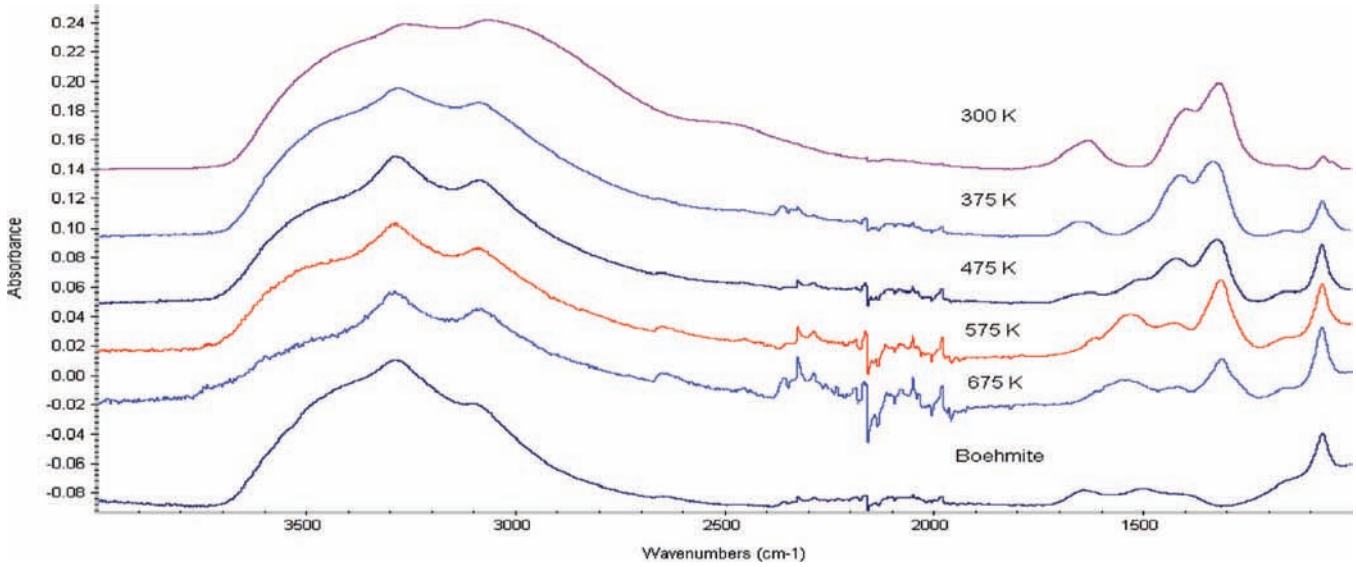

Figure 3. FT-IR spectra of 20% nitric acid on boehmite after heating in vacuum to the temperature given in the figure and cooling to room temperature. A spectrum of commercial boehmite used to prepare the sample is given for comparison. All spectra were taken in air.

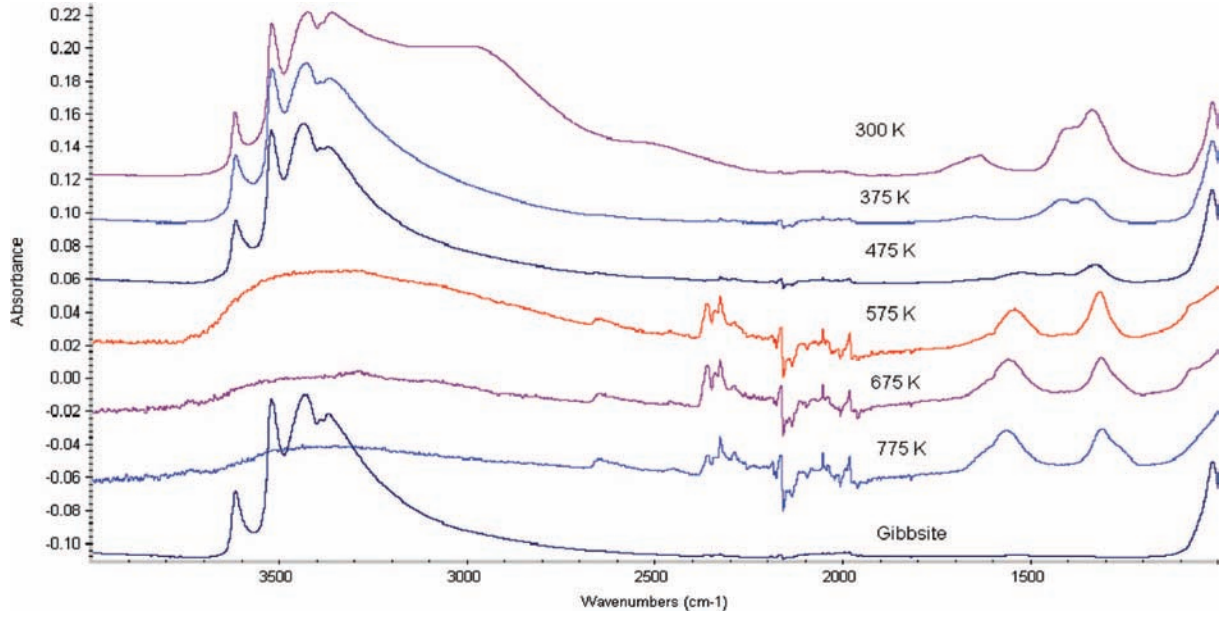

Figure 4. FT-IR spectra of 20% nitric acid on gibbsite after heating in vacuum to the temperature given in the figure and cooling to room temperature. A spectrum of commercial gibbsite used to prepare the sample is given for comparison. All spectra were taken in air.

reported for outer-sphere water-solvated nitrate by Baltrusaitis et al.[12] and were assigned to this species. Since the bands at 1634 (1633) and 3528 cm^{-1} were also observed when only water was placed on the surface, they were assigned as surface-adsorbed water. Although these bands were present in the original sample, their intensity increased, indicating that water was also adsorbed. Although the ν_2 bending mode (1634 cm^{-1}) was red shifted from the frequency of 1645 cm^{-1} reported for water adsorbed on alumina by Goodman et al.,[9] it was in good agreement with the frequency measured for liquid water in a KBr cell (~1635 cm^{-1}). This may indicate that there were several water layers on the boehmite surface producing less interaction with the surface and making the IR spectrum appear more liquid-like. The bands at 2457 and 2991 cm^{-1} were not observed when only water was placed on the surface. Since Reinhardt et al. reported bands at 2670 and 2260 cm^{-1} for $\nu_{1,3}$ of H_3O^+ in the 1:1 amorphous nitric acid/water layer produced by adsorbing nitric acid on ice,[22] it is unlikely these bands are from H_3O^+, but they may be from a larger hydrated proton cluster ($H_{2n+1}O_n^+$) or from hydrogen-bonded interactions between the adsorbed water and the nitrate ion.

The IR spectra observed after heating 20% nitric acid on boehmite in vacuum to temperatures of 375, 475, 575, and 675 K, cooling the sample to room temperature under vacuum, and removing it from the vacuum system to obtain the ATR-FTIR spectrum are presented in Figure 3. A similar temperature profile for 20% gibbsite is presented in Figure 4. Since the intensities of all adsorbed bands decreased significantly as the sample was heated, the scans presented in Figures 3 and 4 have been expanded to full scale to bring out weaker features; therefore, only the band positions are meaningful in these figures. The IR frequencies observed and the assignments for them are also given in Table 1.

Other than a significant decrease in the intensity of the adsorbed nitrate bands caused by loss of over 10% of the adsorbed nitrate, heating the sample to 375 K produced little

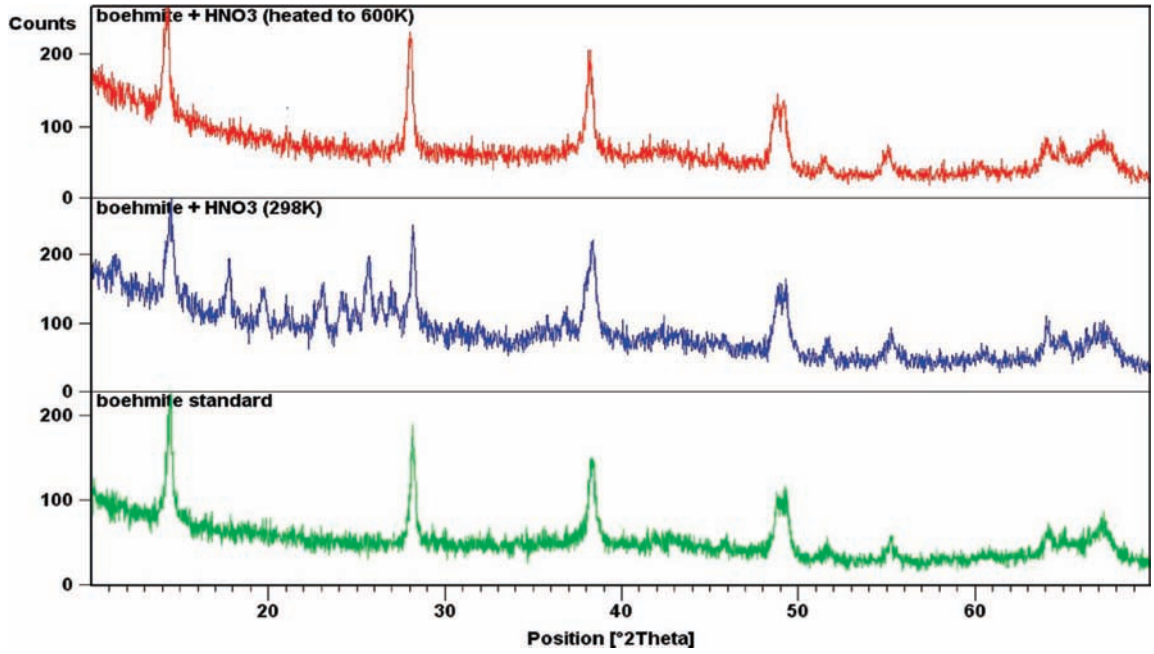

Figure 5. XRD patterns for 36% nitric acid on boehmite at 298 K and after heating to 600 K. The XRD pattern of commercial boehmite used to prepare the sample is given for comparison.

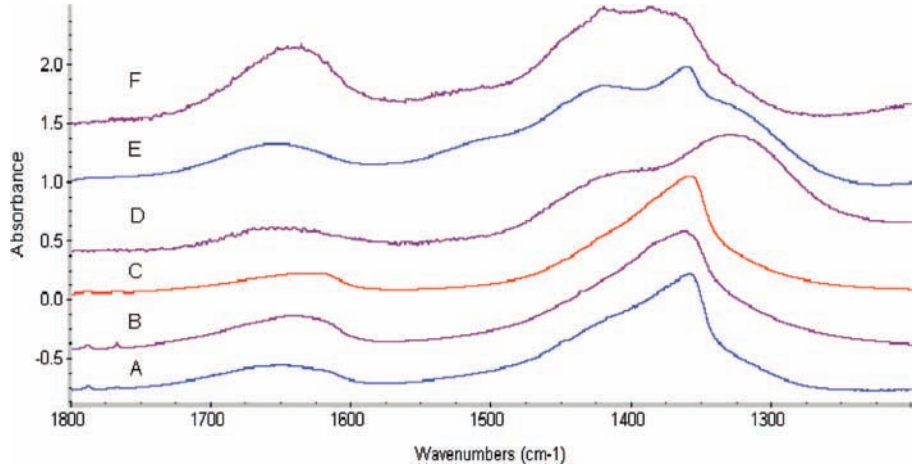

Figure 6. IR spectra observed for (A) 36% nitric acid on boehmite, (B) dried water-soluble product from 36% nitric acid on boehmite, (C) $Al(NO_3)_3 \cdot 9H_2O$, (D) 20% nitric acid on boehmite, (E) $Al(NO_3)_3 \cdot 9H_2O$ dried in air at 350 K for 4 h, and (F) residue from 36% nitric acid on boehmite after washing with water.

change in the spectrum (see Figure 3). There was a slight change in the frequencies observed for the components of the ν_3 NO_3^- band producing a larger splitting. Since Goodman et al.[9] and Baltrusaitis et al.[12] reported that this frequency splitting increased as the amount of adsorbed water on the surface decreased, the increased splitting may have resulted from less water being adsorbed on the surface, and the decrease in the intensity of the 3528 cm^{-1} band supported this conclusion. The band assigned as the ν_2 bending mode of water was now in better agreement with the frequency of this band reported by Goodman et al.[9] for water adsorbed on alumina, which may also be another indication that less water was adsorbed on the surface. Increased splitting could also indicate that the nitrate was interacting more strongly with the surface. There is also some evidence for solvated aluminum hydroxylated nitrate since the 1410 cm^{-1} band has shifted closer to the frequency reported for this species (1416 cm^{-1}).[12]

There were significant changes in the IR spectrum after heating the sample to 475 K. The intensity of the 3528 cm^{-1} band was less than the intensity of this band for the boehmite used to prepare the samples, indicating that the amount of water adsorbed on the surface was less than the amount adsorbed at the typical relative humidity in the laboratory (20−40% RH). For these samples containing less that 3% nitric acid by mass, new bands were observed that were assigned as monodentate and bridged NO_3^- based on the frequencies given by Baltrusaitis et al.[12] The band at 1418 cm^{-1} now clearly indicated that partially solvated aluminum hydroxylated nitrate was present. Further heating caused additional water loss and further frequency shifts, but no additional species were identified.

Similar changes were observed for gibbsite (see Figure 4). Heating to 375 and 475 K in vacuum caused desorption of much of the adsorbed nitric acid and water. The changes in the nitrate region were similar to those observed for nitric acid adsorbed on boehmite. As clearly shown by the loss of the characteristic structure for gibbsite in the OH stretching region, heating the sample over 475 K caused the gibbsite to decompose (see Figure 4). This decomposition has been investigated in detail previously.[23–26] Since the products are a mixture of amorphous alumina and amorphous boehmite,[23–26] the nitrate bands reported for gibbsite

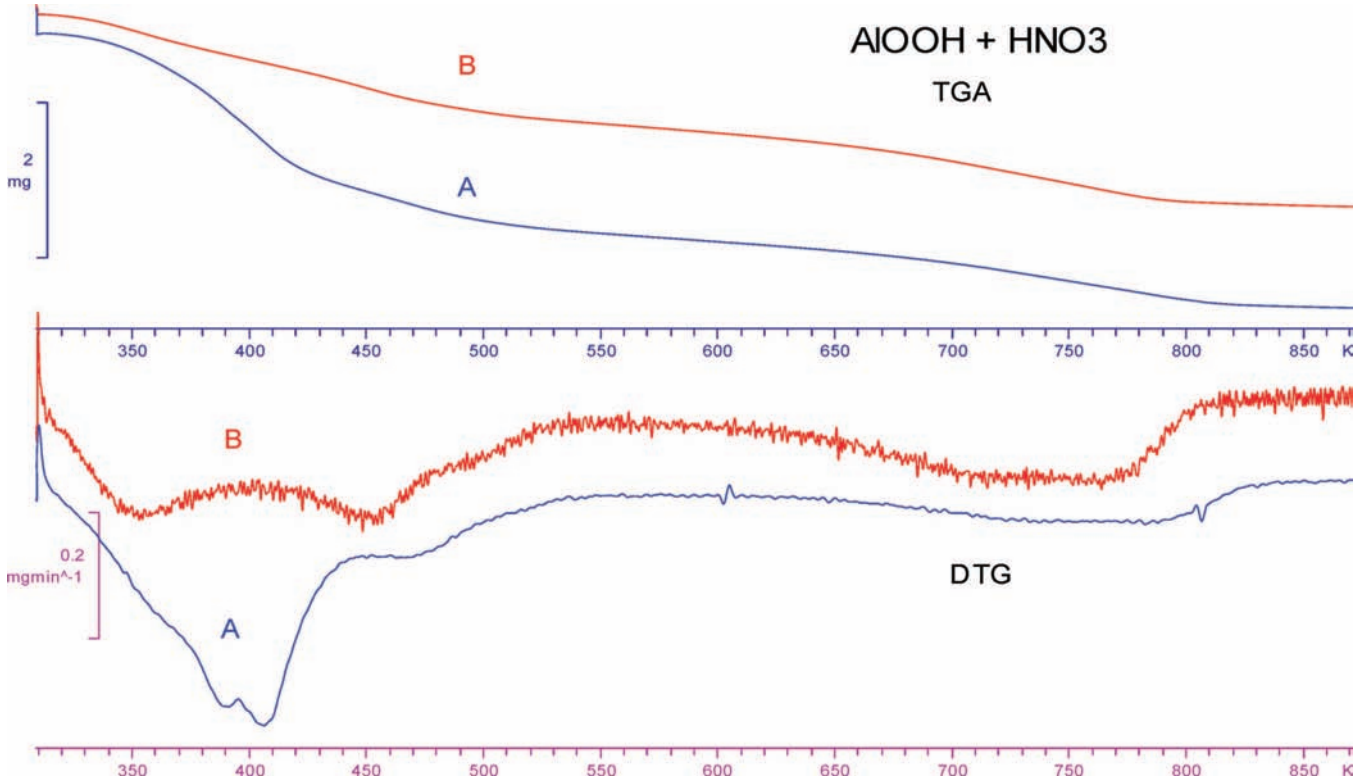

Figure 7. TGA/DTG curves for (A) 20% nitric acid on boehmite and (B) 5% nitric acid on boehmite.

at 675 K in Table 1 are actually for these compounds. Not surprisingly, there was a closer match between the observed frequencies and the frequencies reported previously for alumina since the surface was now more alumina-like.[1–13]

Evidence that nitration had occurred was obtained from the XRD. Although XRD generally only showed the starting material, at least nine diffraction lines that did not correspond to the diffraction pattern of boehmite were observed at $2\theta < 30°$ for 36% nitric acid adsorbed on boehmite prepared by multiple additions of 70% nitric acid solution. This pattern is presented in Figure 5. Although some of the lines could be assigned as $Al(NO_3)_3 \cdot 9H_2O$, the pattern for this compound did not match the pattern of this or any other compound in the data base well enough to make a definite assignment for it. Only the diffraction pattern for boehmite was observed after heating the sample to 600 K. The nitrate remaining on the surface was either amorphous or in too low concentration to be observed by XRD.

Further evidence for nitration of the boehmite was obtained from the IR spectrum observed for 36% nitric acid on boehmite. The strongest band in this spectrum at ~1360 cm^{-1} is similar to the strongest band observed for $Al(NO_3)_3 \cdot 9H_2O$ in frequency and band shape (see Figure 6). Additional evidence for nitration was obtained by placing a sample of 36% nitric acid on boehmite in 10 dm^3 of water. The liquid was decanted into a clean 50 dm^3 beaker and evaporated to dryness at 350 K in a drying oven. The IR spectrum of the white solid that formed had IR bands that also matched the spectrum of $Al(NO_3)_3 \cdot 9H_2O$, indicating that aluminum nitrate had washed off of the surface. The IR spectrum of the residue left after washing indicated that partially solvated aluminum hydroxylated nitrate was still on the surface. As shown in Figure 6D, the IR spectrum observed for 20% nitric acid on boehmite contained no indication of $Al(NO_3)_3 \cdot 9H_2O$. However, when $Al(NO_3)_3 \cdot 9H_2O$ was heated at 350 K, new IR bands formed in the nitrate ν_3 stretching region that were similar to the IR bands observed for 20% nitric acid on boehmite. Since the thermal decomposition of $Al(NO_3)_3 \cdot 9H_2O$ is known to produce alumina through the loss of nitric acid,[27,28] it is not surprising that the process could be reversible and the thermal decomposition of $Al(NO_3)_3 \cdot 9H_2O$ and the adsorption of nitric acid on alumina could pass through similar intermediates.

Temperature-Programmed Desorption (TPD). Thermal gravimetric (TGA) and differential thermal gravimetric (DTG) curves for 20% nitric acid on boehmite and a sample prepared by preheating it at 375 K in vacuum for approximately 1 h (5% nitric acid on boehmite) are presented in Figure 7. The 5% nitric acid had desorption peaks at approximately 350, 450, 725, and 775 K in flowing nitrogen. Since mass losses at 350 and at 775 K were obtained for boehmite that had not been exposed to nitric acid, they are assigned as the desorption of surface-adsorbed species (largely water) and the thermal decomposition of the boehmite, respectively.[29–32] Observation of the 350 K peak suggested that the atmospheric components adsorbed on the surface rapidly once the sample was removed from vacuum. As shown in Figure 8, the EGA-FTIR in vacuum clearly showed that the 450 K peak was from the loss of nitric acid. NO_2 started to evolve at 450 K and peaked at ~675 K. The 725 K peak observed in the TGA is assigned as this desorption since desorptions often peak at lower temperature in vacuum. This assignment is consistent with the EGA-MS results reported by Szanyi et al.[8] who reported a NO_2 desorption peak at 722 K for the decomposition of solvated nitrates. The 350 K desorption was not observed in the EGA-FTIR of samples that had not been exposed to the atmosphere, supporting the assignment that this peak resulted from atmospheric components that adsorbed on the surface after the sample was removed from the vacuum.

As shown in Figure 7, 20% nitric acid on boehmite contained desorption peaks at 390, 410, 450, 725, and 775 K. Over 17% of the sample mass was lost during the first two transitions in

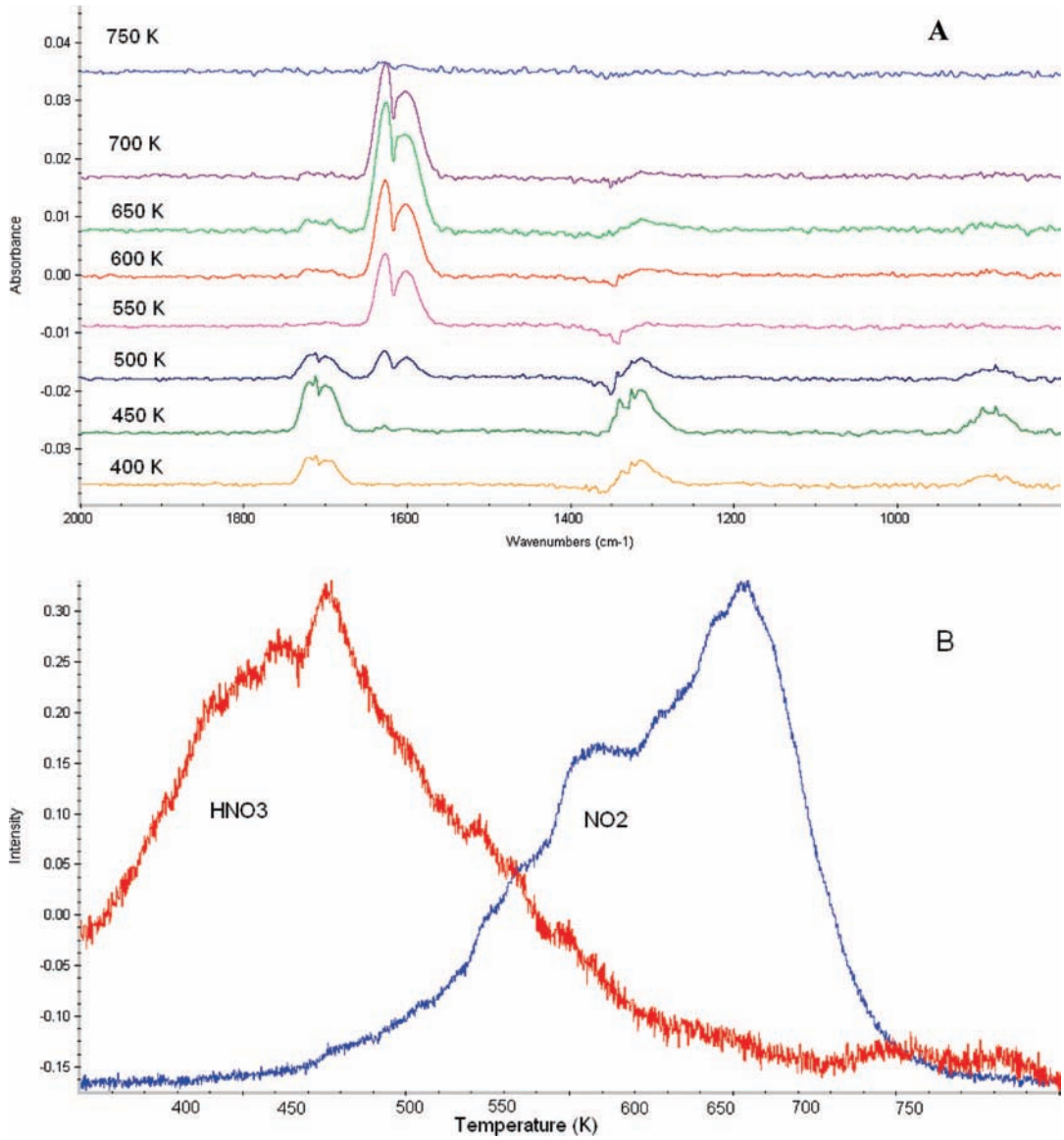

Figure 8. EGA-FTIR spectra (A) and the desorption profiles (B) for HNO_3 and NO_2 observed for the desorption of 5% nitric acid on Boehmite. The bands at and 1710, 1325, and 885 cm^{-1} are from nitric acid. The band at 1620 cm^{-1} is from NO_2. The integrated intensities of the bands at 1710 and 1620 cm^{-1} were used to generate these profiles. Different scale expansions are used for HNO_3 and NO_2 in the desorption profiles to bring out the shape of the curves.

flowing nitrogen. EGA-FTIR indicated that the mass loss at 390 K resulted from the vaporization of water and nitric acid, the loss at 410 K was largely from nitric acid, the loss at 450 K was from a mixture of HNO_3 and NO_2, and the loss at 725 K was from NO_2 (see Figure 9). Approximately 2.9% of the sample mass was lost in the 450/725 K steps. The differences between the two patterns coupled with the IR spectral data presented above indicated that the 390 and 410 K transitions were from the loss of the hydrated nitrate, the 450 K transition was most likely from partially hydrated aluminum hydroxylated nitrate, and the 725 K transition was from the coordinated nitrate. Since AlOOH also decomposed in this temperature region, the decomposition of coordinated nitrate corresponded to the decomposition of hydrated nitrate on alumina reported by Szanyi et al.[8]

TGA and DTG observed for 18% nitric acid adsorbed on gibbsite are presented in Figure 10. This sample, which was prepared by reacting the gibbsite with 1 mL of 70% nitric acid solution, had a 14.8% mass loss by 420 K and an additional 2.5% mass loss by 475 K. The $Al(OH)_3$ decomposed at 475 K, making it difficult to determine if there was additional nitrate desorption. Heating this sample to 375 K in vacuum removed the 420 K desorption, but the 2.5% mass loss at 475 K was still present. The shoulder at 570 K observed in the 18% sample was not present in the 2.5% by mass sample. This difference may have resulted from a secondary reaction between the nitric acid and the decomposing $Al(OH)_3$ since the 18% nitric acid would have more residual nitric acid vapor in the cell.

EGA indicated that the initial mass loss for 18% nitric acid on gibbsite was from desorption of nitric acid and water (see Figure 11). Nitric acid loss began at 335 K and had a maximum desorption rate at 395 K. There was an indication of a second nitric acid desorption at 510 K. Water had peak desorbtions at 325 K, with the initial nitric acid desorption at 395 K, and at 560 K. The two initial desorptions were from water adsorbed on the surface. The large desorption at 560 K was from the thermal decomposition of the $Al(OH)_3$.[23–26] Although small amounts of NO_2 desorbed with the nitric acid at 395 and 500 K, the main NO_2 desorptions were at 650 and 725 K. The 725 K desorption agreed with the final NO_2 desorption observed on

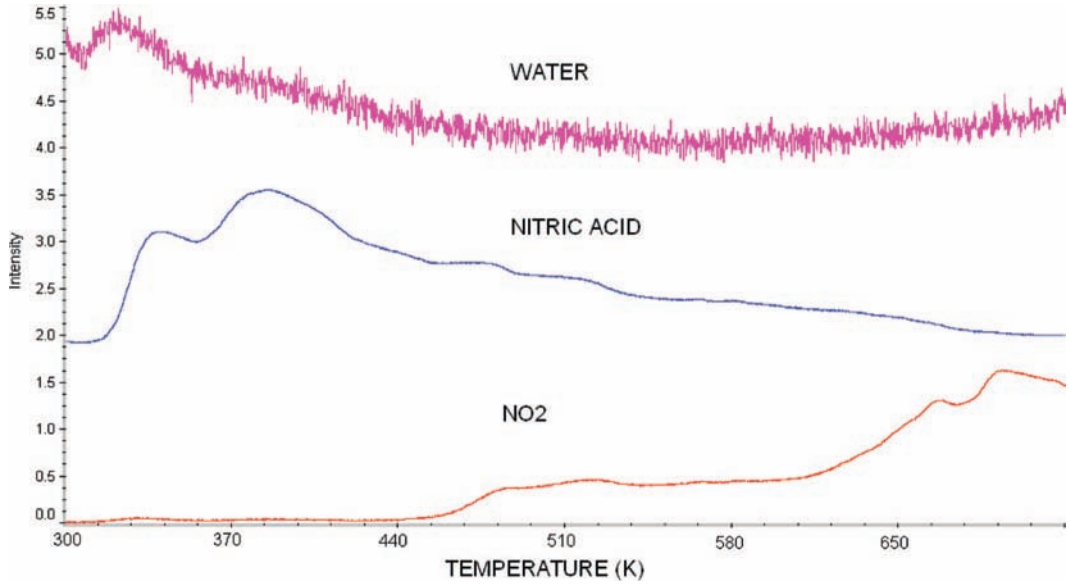

Figure 9. The profiles observed for the desorption of 36% nitric acid on boehmite prepared by adding additional nitric acid solution to 20% nitric acid on boehmite. The integrated intensities of the bands for H_2O at 3500 cm^{-1}, HNO_3 at 1710 cm^{-1}, and NO_2 at 1620 cm^{-1} were used to generate these profiles. Different scale expansions were used to bring out the shape of the curves.

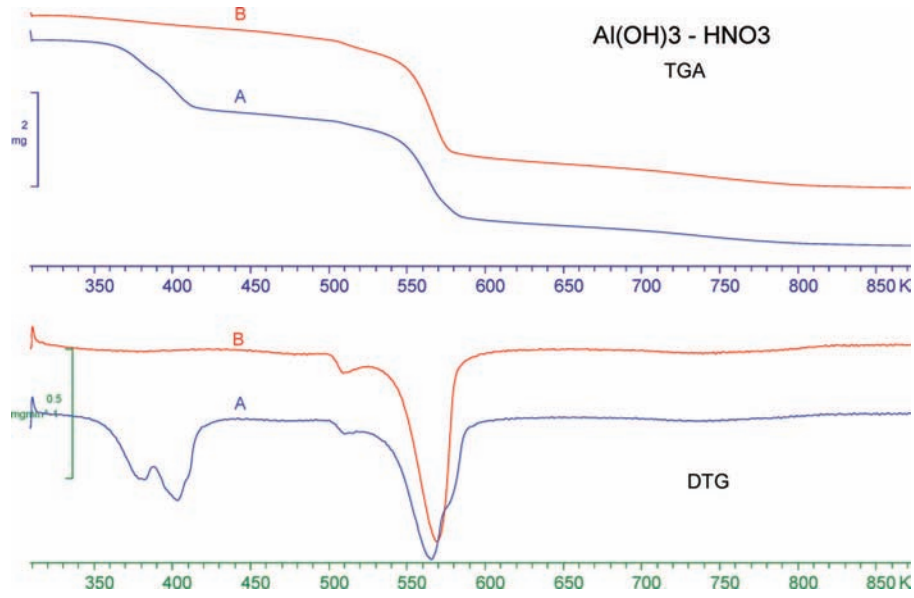

Figure 10. TGA/DTG curves for (A) 18% nitric acid on gibbsite and (B) 2.5% nitric acid on gibbsite.

boehmite and was assigned as this transition since amorphous boehmite formed during the gibbsite decomposition. The 650 K may be desorption from the amorphous alumina that was also formed during the gibbsite decomposition. As shown in Figure 11, all of the 395 K water and nitric acid desorptions were removed by heating the 18% sample to 375 K for 60 min in vacuum to prepare 3% nitric acid on gibbsite. The only nitric acid desorption from this sample was centered at around 500 K, and the only water desorption was the $Al(OH)_3$ decomposition at 560 K. The NO_2 desorption curve showed a larger peak at 500 K than the 18% sample and also evolved with the water at 560 K. The peak at 650 K was not observed in this sample, a result consistent with the lack of a high-temperature shoulder in the TGA for this sample. The shape and the desorption temperatures for the 395 K desorption were similar to the initial desorption observed for 20% nitric acid on boehmite and were assigned as desorption of outer-sphere hydrated nitrate. This desorption is actually a double peak, which is consistent with the conclusion by Baltrusaitis et al.[12] that two forms of hydrated nitrate were present on the surface. The 500 K desorption probably corresponded to the 450 K peak observed for nitric acid/boehmite. The temperature difference indicated that partially hydrated aluminum hydroxylated nitrate was more strongly bonded to the gibbsite surface, suggesting that the chemical formulas of these compounds are slightly different.

Differential Scanning Calorimetry (DSC). DSC observed for samples used in the TGA experiments are presented in Figure 12. Endothermic transitions were observed that corresponded to each mass loss in the TGA. The assignments for these transitions are discussed above. There were three highly overlapped endothermic transitions in the nitric acid desorption region for 20% nitric acid on boehmite and two clear transitions for the 18% nitric acid on gibbsite, indicating that there was more than one type of binding of nitric acid to each surface. These thermal events were not observed after heating the sample to 375 K to produce the 3−5% samples. No exothermic transitions were observed for either sample, suggesting that the

adsorbed nitrate did not strongly react with the surface as the sample was heated.

Enthalpy of Adsorption. Although it should be possible to determine the enthalpy of adsorption for each transition from the DSC data, neither the initial sample composition nor the composition of the evolving vapor was known with enough precision to permit accurate binding enthalpies to be calculated using only this method. In an attempt to better determine these values, the evolution profiles of nitric acid for 20% nitric acid using TGA data and for 5% nitric acid samples not exposed to air using EGA data were analyzed using the direct method given by Brown[33] and the curve fitting method given by Spinicci.[34] Both methods express the rate expression in terms of the extent of reaction (α). The extent of reaction can be calculated from TGA data using

$$\alpha = (m_0 - m_t)/(m_0 - m_f) \quad (1)$$

where m_0 is the initial sample mass, m_t is the sample mass at time t, and m_f is the final sample mass or from EGA-FTIR data using

$$\alpha = A_t/A_f \quad (2)$$

where A_t is the total sample absorbance up to time t and A_f is the total sample absorbance at the completion of the process. For most desorption processes, the rate expression is given by

$$d\alpha/dT = k(1 - \alpha)^n \quad (3)$$

where n is usually 1 or 2. For reversible processes, Spinicci determined that k was related to the enthalpy of desorption ($\Delta_{DES}H$) by[34]

$$k = \text{const} \cdot \exp(-(\Delta_{DES}H/RT) \quad (4)$$

Substituting eq 4 into eq 3, rearranging, and taking logarithms gives

$$\ln[d\alpha/dT/(1 - \alpha)^n] = -(\Delta_{DES}H/RT + \ln(\text{const}) \quad (5)$$

A plot of $\ln[d\alpha/dT/(1 - \alpha)^n]$ verses $1/T$ should yield a straight line with slope $= -(\Delta_{DES}H/R$. The linearity of the plot is used to determine the correct order of reaction (n).

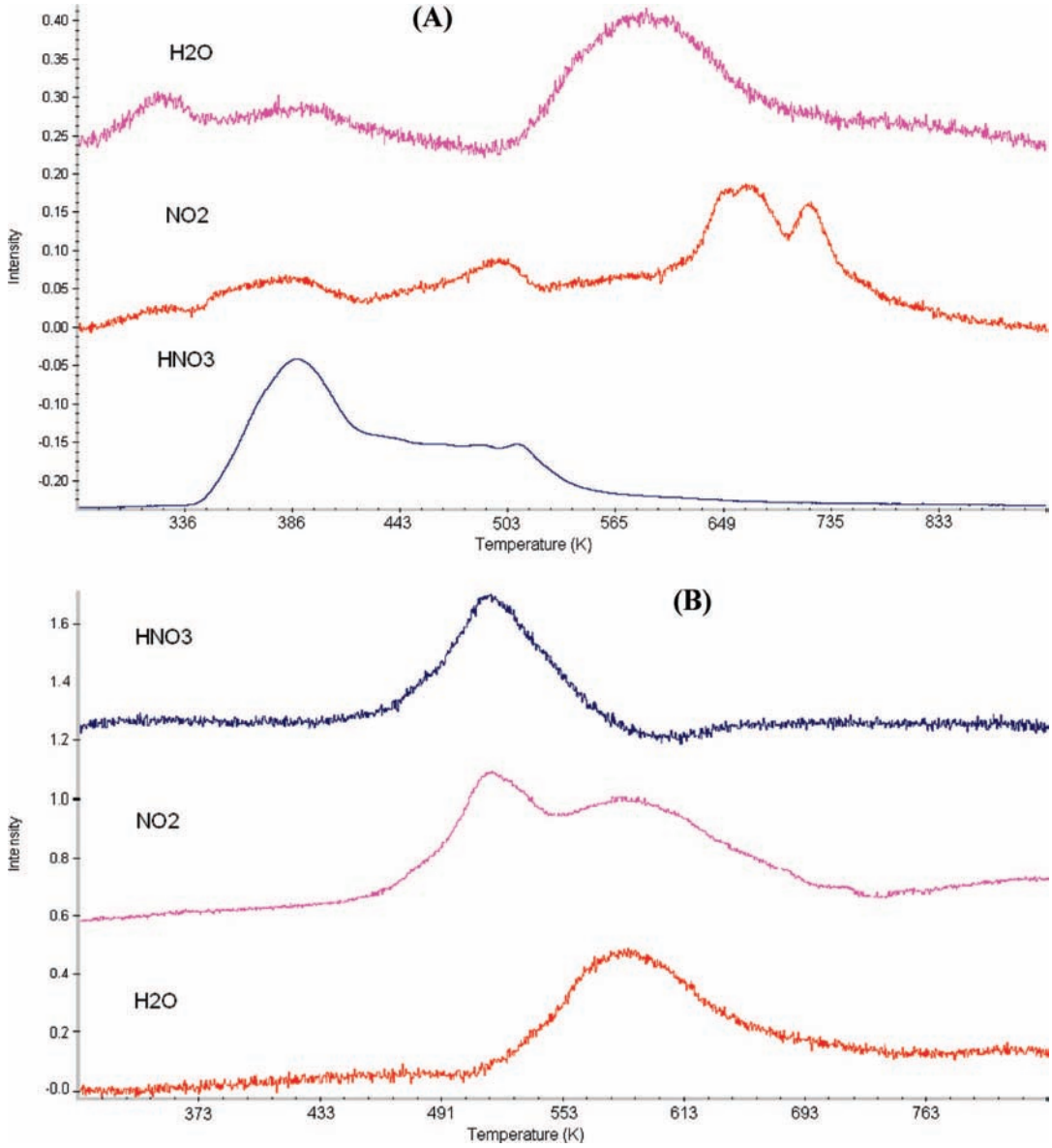

Figure 11. Vacuum TPD patterns for (A) 18% nitric acid adsorbed on gibbsite and (B) 2.5% nitric acid on gibbsite. The intensity of each pattern has been expanded to full scale to show the shape of the curves.

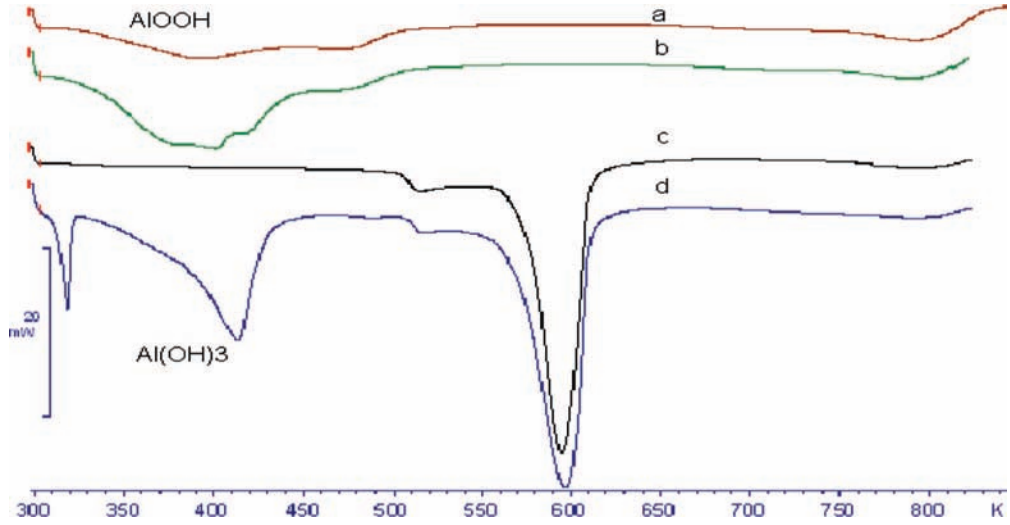

Figure 12. The DSC observed for (a) 5% nitric acid adsorbed on boehmite, (b) 20% nitric acid adsorbed on boehmite, (c) 2.5% nitric acid on gibbsite, and (d) 18% nitric acid on gibbsite.

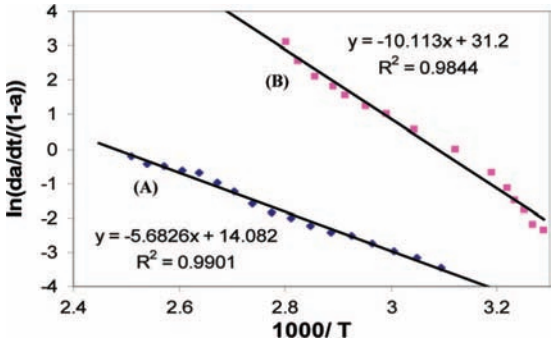

Figure 13. A plot of ln [dα/dT/(1 − α)^n] verses 1/T for the desorption of (A) 20% nitric acid on boehmite and (B) 5% nitric acid on boehmite. Curve (A) was generated using TGA data, and (B) was from EGA data for the TPD curve of nitric acid.

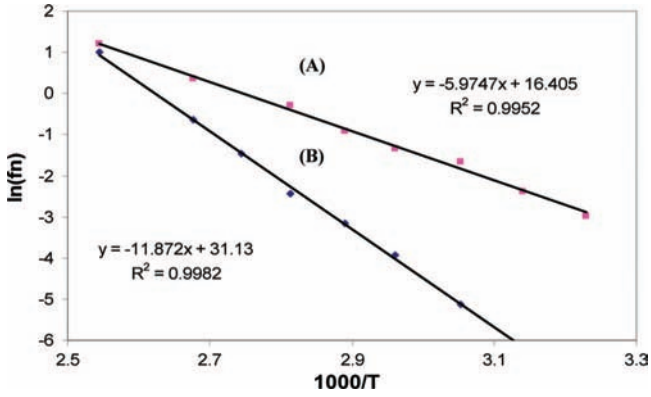

Figure 14. Van't Hoff plots for the desorption of nitric acid from (A) 20% nitric acid on gibbsite and (B) 5% nitric acid on gibbsite determined using pseudo-Knudsen conditions.

Examples of the kinetic plots obtained using this approach for the 350 K desorption of nitric acid from 20% nitric acid on boehmite and from 5% nitric acid on boehmite using the nitric acid signal to calculate α are given in Figure 13. The best fit for each sample was obtained by using $n = 1$, indicating that the evolution followed the first-order desorption model. The 20% sample had an enthalpy of desorption of 45 ± 10 kJ/mol while the 5% sample had an enthalpy of desorption of 85 ± 10 kJ/mol. These transitions are assigned as desorption of nitric acid from outer-sphere hydrated nitrate and from hydrated aluminum hydroxylated nitrate, respectively.

An example of the van't Hoff plots obtained using the constant temperature TGA procedure described in the Experimental Section for the desorption of nitric acid from gibbsite is shown in Figure 14. The initial desorption for the 18% nitric acid sample had an enthalpy of desorption of 50 ± 10 kJ/mol. The 5% nitric acid sample had an enthalpy of desorption of 95 ± 10 kJ/mol.

The enthalpy change determined for outer-sphere hydrated nitrate was between 45 and 55 kJ/mol, depending upon the method used to determine it. This value is slightly larger than the enthalpy change calculated for the vaporization of nitric acid

$$HNO_3(l) \leftrightarrow HNO_3(g) \quad (6)$$

using the enthalpy of formation data tabulated by Wagman et al.[35] or using the vapor pressure measurements for liquid nitric acid reported by Duisman and Stern[36] (39 kJ/mol), but it agrees within experimental error with the enthalpy of vaporization calculated for 60−80% nitric acid in water using the vapor pressure data of Sproesser and Taylor[37] (45−48 kJ/mol). The similarity of these values indicates that this process can be reasonably modeled as the vaporization of nitric acid solution from the surface.

Since the IR spectrum observed after heating to 375 K was consistent with the IR spectrum reported for partially hydrated aluminum hydroxylated nitrate,[12] this was assumed to be the main species on the surface. The enthalpy of desorption determined for this species was 85 ± 10 and 95 ± 10 kJ/mol for boehmite and gibbsite, respectively. This small difference may result from the differences in surface composition. The nitrate could form from the reaction between surface hydroxyls and nitric acid. Upon heating, a proton transfer (probably from the water of hydration) could re-form the nitric acid and the mineral in a process similar to the low-temperature decomposition reported for aluminum nitrate nonohydrate.[27,28]

EGA-FTIR spectra indicated that the coordinated nitrate desorbed as NO_2. While it could not be observed in the IR, O_2 must also desorb to maintain mass/charge balance. Since gibbsite decomposed to form a mixture of boehmite and amorphous alumina starting at 475 K,[29–32] all of the analysis for NO_2 desorption was done using boehmite samples. The main NO_2 desorption was between 575 and 775 K. Fitting this profile for the EGA-FTIR data using the procedure given by Brown[33] produced an apparent enthalpy of desorption of 55 kJ/mol NO_2

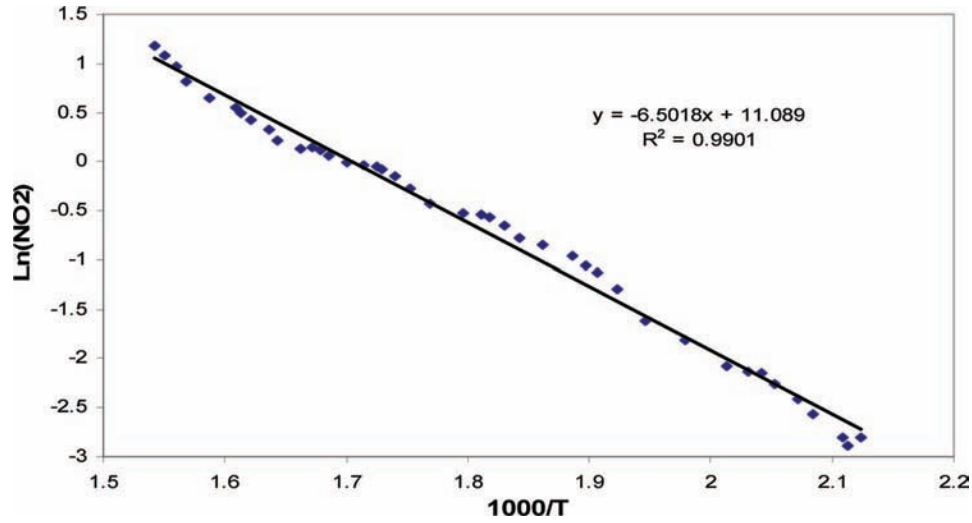

Figure 15. Fit for the release of nitrogen dioxide using the first-order desorption model. The enthalpy change determined for this process is 55 ± 10 kJ/mol.

using the first-order desorption model (see Figure 15). Since the NO_2 desorption profile was nearly identical to the NO_2 desorption profile reported for the thermal decomposition of $Mg_{1-x}Al_xO(NO_3)_x$ by Xu and Zeng,[38] it was reasonable to assume that similar processes were occurring for both systems. Since the final desorption for $Mg_{1-x}Al_xO(NO_3)_x$ was from nitrate coordinated to aluminum, a reasonable model of this decomposition would be

$$Al_2O_2(NO_3)_2 \leftrightarrow Al_2O_3 + 2NO_2 + 0.5O_2 \quad (7)$$

On the basis of the measured enthalpy of reaction and data tabulated by Wagman et al,[35] the enthalpy of formation of $Al_2O_2(NO_3)_2$ was calculated to be −1675 kJ/mol. However, the enthalpies of formation for aluminum nitrate ($Al(NO_3)_3$ = −1155 kJ/mol),[35] copper nitrate ($Cu(NO_3)_2$ = −303 kJ/mol),[35] or calcium nitrate ($Ca(NO_3)_2$ = −938 kJ/mol)[35] are larger than that of the corresponding oxide. Since the value determined for $Al_2O_2(NO_3)_2$ was less than the corresponding oxide, a better representation may be $Al_2O_2(OH)NO_3$. This would be more consistent with adsorption on boehmite and the assignment by Szanyi et al. that the 725 K desorption was from hydrated nitrate.[8] One possible thermal decomposition reaction that would generate NO_2

$$2Al_2O_2(OH)NO_3 \leftrightarrow Al_2O_2(OH)_2 + Al_2O_3 + 2NO_2 + 0.5O_2 \quad (8)$$

produced an estimated enthalpy of formation for $Al_2O_2(OH)NO_3$ of −1835 kJ/mol, a value more consistent with $\Delta_f H$ values observed for other nitrates.

Conclusions

Samples containing up to 36% nitrate/water by mass were prepared by mixing boehmite or gibbsite with 70% nitric acid solution. IR indicated that most of the adsorbed nitrate was in the form of outer-sphere water-solvated nitrate that desorbed as nitric acid with an enthalpy of desorption (~45 kJ/mol) similar to the enthalpy of vaporization for a 60−80% nitric acid solution (45−48 kJ/mol). Since the values were similar for both boehmite and gibbsite, this value should also be a reasonable estimate for the desorption enthalpy for solvated nitrate on alumina.

Approximately 5% of the total mass was adsorbed nitrate after heating in vacuum at 375 K for 60 min. The IR spectrum of 5% nitrate was consistent with the spectrum for partially solvated aluminum hydroxylated nitrate. This compound desorbed as nitric acid and had an enthalpy of desorption of 85−95 kJ/mol. The composition of the surface may have influenced the desorption enthalpy for this species since gibbsite had a slightly larger enthalpy of desorption than did boehmite. The nitric acid may have formed from a reaction between the adsorbed water and the nitrate in a process similar to the low-temperature thermal decomposition of $Al(NO_3)_3 \cdot 9H_2O$.[26,27]

Nitrate bands were observed after heating the sample to ~700 K in vacuum, indicating that there were also more stable nitrate species formed. The IR spectra observed for this coordinated nitrate were consistent with the spectra observed for monodentate and bridged nitrate. This nitrate desorbed as nitrogen dioxide. The similarity of the desorption profile to that observed for $Mg_{1-x}Al_xO(NO_3)_x$ by Xu and Zeng[36] supported their conclusion that the NO_2 evolution was from nitrate bonded to aluminum. The enthalpy of formation determined was realistic for a hydroxyl nitrate such as $Al_2O_2(OH)NO_3$, indicating that this compound may also be the hydrated nitrate reported by Szanyi et al.[8]

Repeated applications of nitric acid produced a water-soluble aluminum nitrate that could be removed by washing with water. While the species observed with less than 20% nitric acid on the surface were clearly not $Al(NO_3)_3 \cdot 9H_2O$, changes in the IR spectrum in the ν_3 nitrate stretching region of $Al(NO_3)_3 \cdot 9H_2O$ as it was heated in air at 350 K suggested that similar intermediates were formed in the low-temperature thermal decomposition of $Al(NO_3)_3 \cdot 9H_2O$ and the nitration of boehmite.

These results indicated that boehmite and gibbsite will strongly adsorb nitrates on the surface, permanently removing them from the atmosphere. They can also adsorb several additional layers as hydrated nitrate in humid environments. These layers have similar vaporization properties as nitric acid solution and could provide a mechanism for the transport of nitric acid though the environment. Mashburn et al. reported that Na montmorillonite adsorbed nitric acid more rapidly when hydrated and could contain ~30% HNO_3 by mass at 44% relative humidity.[39] Boehmite appears to have similar capacities, making it an efficient sink for nitric acid. Although gibbsite

does not adsorb as much nitric acid, it is at least as effective as alumina in removing nitric acid. Kelly et al. reported that adding soluble components to the surface of insoluble particles increased the cloud condensation nuclei (CCN).[40] Since nitric acid reacted to form soluble aluminum nitrate on the surface, hydrated nitrate could enhance the CCN of these particles and affect rainfall patterns.

Acknowledgment. The authors are grateful to the JMU Dean's Scholarship fund for providing support for M. Ross, The National Science Foundation, MRI/RUI #0340245, for providing the TGA and DSC used in this project, the National Science Foundation, DMR #0315345, for providing the XRD unit used in this project, and the National Science Foundation Research Experiences for Undergraduates Award #0353807 and the U.S. Department of Defense ASSURE program, Grant #0353773, for providing additional support for this project.

References and Notes

(1) Seinfeld, J. H. *Atmospheric Chemistry and Physics of Air Pollution*; John Wiley and Sons: New York, 1986.
(2) Sillman, S.; Logan, J. A.; Wofsy, S. C. *J. Geophys. Res.* **1990**, *95*, 1837.
(3) Dentener, F. J.; Carmichael, G. R.; Zhang, Y.; Lelieveld, J.; Crutzen, P. J. *Geophys. Res.* **1996**, *101*, 22869.
(4) Venkov, T.; Hadjiivanov, K.; Klissurski, D. *Phys. Chem. Chem. Phys.* **2002**, *4*, 2443.
(5) Westerberg, B.; Fridell, E. *J. Mol. Catal. A: Chem.* **2001**, *165*, 249.
(6) Haung, S.-J.; Walters, A. B.; Vannice, M. A. *Appl. Catal., B* **2000**, *26*, 101.
(7) Goodman, A. L.; Miller, T. M.; Grassian, V. H. *J. Vac. Sci. Technol., A* **1998**, *16*, 2585.
(8) Szanyi, J.; Kwak, J. H.; Chimentao, R. J.; Peden, C. H. F. *J. Phys. Chem. C* **2007**, *111*, 2661.
(9) Goodman, A. L.; Bernard, E. T.; Grassian, V. H. *J. Phys. Chem. A* **2001**, *105*, 6443.
(10) Borensen, C.; Kirchner, U.; Scheer, V.; Vogt, R.; Zellner, R. *J. Phys. Chem. A* **2000**, *104*, 5036.
(11) Seisel, S.; Borensen, C.; Vogt, R.; Zellner, R. *Phys. Chem. Chem. Phys.* **2004**, *6*, 5498.
(12) Baltrusaitis, J.; Schuttlefield, J.; Jensen, J. H.; Grassian, V. H. *Phys. Chem. Chem. Phys.* **2007**, *9*, 4970.
(13) Underwood, G. M.; Li, P.; Al-Abadleh, H.; Grassian, V. H. *J. Phys. Chem. A* **2001**, *105*, 6609.
(14) Grassian, V. H. *Int. Rev. Phys. Chem.* **2001**, *20*, 467.
(15) Grassian, V. H. *J. Phys. Chem. A* **2002**, *106*, 860.
(16) Vlasenko, A.; Sjogren, S.; Weingartner, E.; Stemmler, K.; Gaggeler, H. W.; Amman, M. *Atmos. Chem. Phys.* **2006**, *6*, 2147.
(17) Angelini, M. M.; Garrad, R. J.; Rosen, S. J.; Hinrichs, R. Z. *J. Phys. Chem. A* **2007**, *111*, 3326.
(18) For example, see: Atkins, P. W.; DePaula, J. *Physical Chemistry*, 8th ed.; Freeman, 2006; p 756.
(19) DeVore, T. C.; Gallaher, T. N. *Inorg. Chem.* **1984**, *23*, 3506.
(20) Rhoten, M. C.; DeVore, T. C. *Chem. Mater.* **1997**, *9*, 1757.
(21) Crouch, M. A.; DeVore, T. C. *Chem. Mater.* **1996**, *8*, 36.
(22) Reinhardt, H.; Fida, M.; Zellner, R. J. *Mol. Struct.* **2003**, *661*, 567.
(23) Candela, L.; Perlmutter, D. D. *Ind. Eng. Chem. Res.* **1992**, *31*, 694.
(24) Gong, X. Y.; Nie, Z. M.; Qian, M. X.; Liu, J.; Pederson, L. A.; Hobbs, D. T.; McDuffle, N. G. *Ind. Eng. Chem. Res.* **2003**, *42*, 2163.
(25) Whittington, B.; Ilievski, D. *Chem. Eng. J.* **2004**, *98*, 89.
(26) Wang, H. P.; Xu, B. G.; Smith, P.; Davies, M.; DeSilva, L.; Wingate, C. *J. Phys. Chem. Solids* **2006**, *67*, 2567.
(27) Tsuchida, T.; Furuich, R.; Ishii, T. *Thermochim. Acta* **1980**, *39*, 103.
(28) Pacewska, B.; Keshr, M. *Thermochim. Acta* **2002**, *385*, 73.
(29) El-Shereafy, E.; Abousekkina, M. M.; Mashaly, A.; El-Ashry, M. *J. Radioanal. Nucl. Chem.* **1998**, *237*, 183.
(30) Stacy, M. H. *Langmuir* **1987**, *3*, 681.
(31) Alphonse, P.; Courty, M. *Thermochim. Acta* **2005**, *425*, 75.
(32) Percharroman, C.; Sobrados, I.; Iglesias, J. E.; Gonzalez-Carrero, T.; Sanz, J. *J. Phys. Chem. B* **1999**, *103*, 6160.
(33) Brown, M. E. *Introduction to Thermal Analysis*; Chapman & Hall: New York, 1988.
(34) Spinicci, R. *Thermochim. Acta* **1997**, *296*, 87.
(35) Wagman, D. D.; Evans, W. H.; Parker, V. B.; Schumm, R. H.; Halow, I.; Bailey, S. M.; Churney, K. L.; Nuttall, R. L. *J. Phys. Chem. Ref. Data*, Supplement No. 2;American Chemical Society, **1982**, Vol. 11.
(36) Duisman, J. A.; Stern, S. A. *J. Chem. Eng. Data* **1969**, *14*, 457.
(37) Sproesser, W. C.; Taylor, G. B. *J. Am. Chem. Soc.* **1921**, *43*, 1782.
(38) Xu, Z. P.; Zeng, H. C. *Chem. Mater.* **2001**, *13*, 4564.
(39) Mashburn, C. D.; Frinak, E. K.; Tolbert, M. A. *J. Geophys. Res. D: Atmos.* **2006**, *15*, D152313.
(40) Kelly, J. T.; Chuang, C. T.; Wexler, A. S. *Atmos. Environ.* **2007**, *41*, 2904.

JP7110555